iScience

CellPress
OPEN ACCESS

Article

Moderate intensity exercise may protect cardiac function by influencing spleen microbiome composition

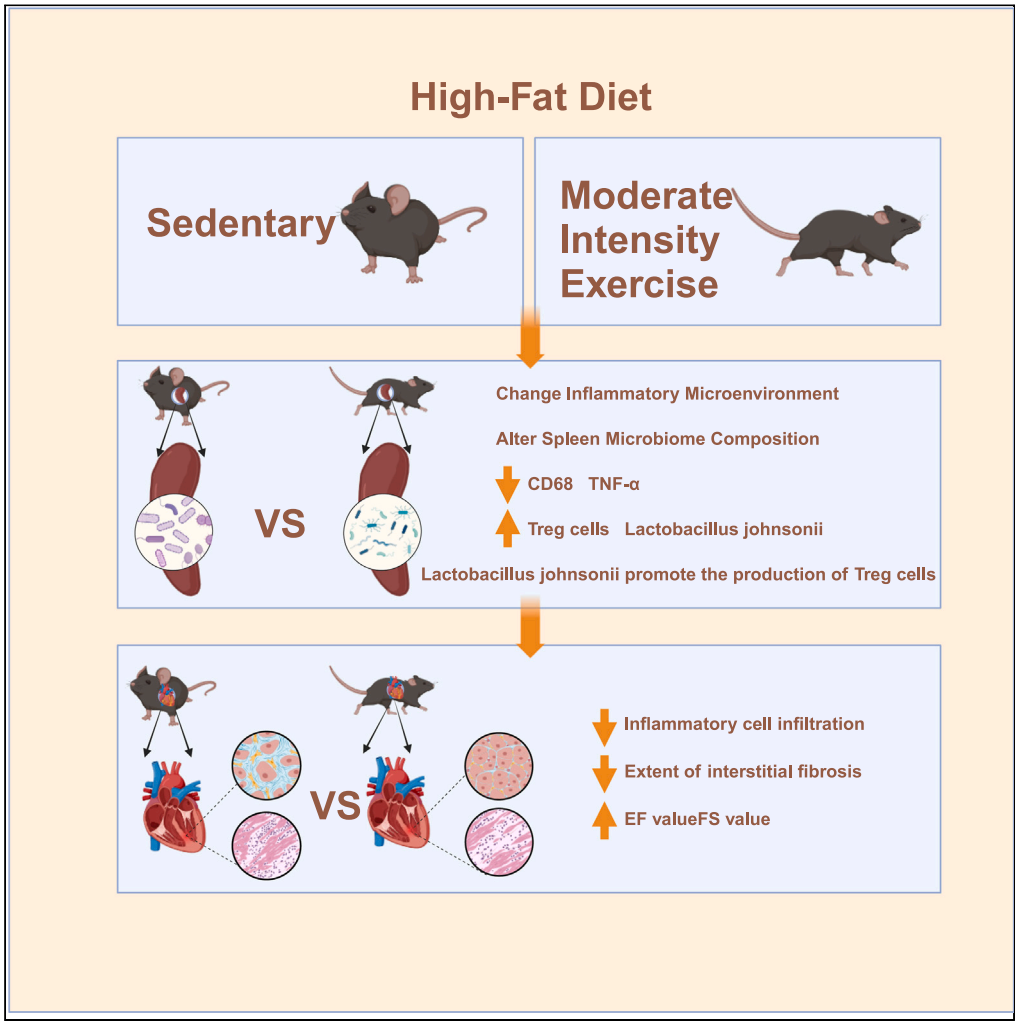

Jie Xiao, Xing Chen, Weina Guo, Yang Li, Jinping Liu

liujinping@znhospital.cn

Highlights

Mice spleen contained a diverse array of microbiotas

Different intensities exercise alters the compositions of the spleen microbiome

Lactobacillus johnsonii may contribute to the production of Treg cells

Xiao et al., iScience *27*, 108635
February 16, 2024
https://doi.org/10.1016/j.isci.2023.108635

iScience

CellPress
OPEN ACCESS

Article

Moderate intensity exercise may protect cardiac function by influencing spleen microbiome composition

Jie Xiao,[1,2,3,5] Xing Chen,[1,2,3,5] Weina Guo,[4,5] Yang Li,[1,2,3] and Jinping Liu[1,2,3,6,*]

SUMMARY

The beneficial effects of physical exercise on human cardiorespiratory fitness might be through reduced systemic inflammation, but the mechanism remains a controversy. Recent studies have highlighted the importance of spleen microbiomes in immune regulation. Hence, we conducted a study using a high-fat diet and exercise mouse model to investigate the relationships among different exercise intensities, spleen microbiome composition, and cardiac function. The mice spleen contained a diverse array of microbiota. Different intensities of exercise resulted in varying compositions of the spleen microbiome, Treg cell levels, and mouse heart function. Additionally, the abundance of *Lactobacillus johnsonii* in the mouse spleen exhibited a positive correlation with Treg cell levels, suggesting that *Lactobacillus johnsonii* may contribute to the production of Treg cells, potentially explaining the protective role of moderate-intensity exercise on cardiac function. In conclusion, our findings provide evidence that moderate-intensity exercise may promote cardiac function protection by influencing the spleen microbiome composition.

INTRODUCTION

According to the American Heart Association's (AHA) annual report[1] and the annual report on cardiovascular health and disease in China 2021,[2] cardiovascular diseases (CVDs) are the leading cause of mortality worldwide. Considerable evidence has underscored the positive impact of physical exercise on cardiovascular diseases, including the reduction of cardiovascular risk factors, mitigation of cardiovascular events, enhancement of cardiorespiratory fitness, and lowered rates of all-cause mortality and mortality related to cardiovascular diseases.[3,4] The potential mechanisms responsible for the protective effects of physical exercise in cardiovascular diseases include reducing myocardial oxidative stress, promoting physiological cardiac hypertrophy, and inducing vascular responses, cardiac metabolic adaptations, and systemic immune responses.[5] In particular, a significant advantage of regular exercise is its ability to effectively mitigate chronic systemic inflammation, which is strongly implicated in the development and progression of cardiovascular diseases[6]; however, the underlying mechanism remains a subject of controversy and requires further clarification.

The spleen, being the largest and most essential immune organ, has received increasing attention for its critical role in modulating immune balance in both humans and rodents.[7] Carnevale et al. presented compelling evidence that underscores the spleen's pivotal role as a central hub connecting the nervous and immune systems, particularly in the context of cardiovascular and metabolic diseases.[7] Lembo et al. discovered that placental growth factor (PIGF) facilitates a neuroimmune interaction within the spleen, leading to the onset of hypertension.[8] Potteaux et al. demonstrated that angiotensin II mobilizes spleen monocytes, which in turn promote the development of abdominal aortic aneurysm in ApoE$^{-/-}$ mice.[9] These results demonstrate the pivotal role of the spleen in the development of cardiovascular diseases. Furthermore, a recent study shed light on the impact of exercise on the spleen.[10] However, whether exercise exerts a protective role on cardiac function via the spleen remains to be clarified.

Tissue resident microbiomes have gained increased attention in current studies. Multiple compelling studies have demonstrated the presence of the microbiome in various tissues, including adipose tissue,[11] kidney,[12] liver,[13] brain,[14] tumors,[15] and other tissues.[16,17] The microbiome may be associated with the progression of diseases. Recently, a novel concept highlighted the pivotal role of the spleen resident microbiome in disease progression within the experimental autoimmune encephalomyelitis (EAE) mouse model.[18] *Enterobacter* was enriched in the spleens of the EAE group, and oral inoculation of live *Enterobacter* sp. significantly accelerated the clinical scores of EAE mice. However, few studies have investigated the relationship between physical exercise and the spleen microbiome. Herein, we conducted a study to

[1]Department of Cardiovascular Surgery, Zhongnan Hospital of Wuhan University, Wuhan 430071, China
[2]Hubei Provincial Engineering Research Center of Minimally Invasive Cardiovascular Surgery, Wuhan 430071, China
[3]Wuhan Clinical Research Center for Minimally Invasive Treatment of Structural Heart Disease, Wuhan 430071, China
[4]Department of Obstetrics and Gynecology, Union Hospital, Tongji Medical College, Huazhong University of Science and Technology, Wuhan 430022, China
[5]The authors contributed equally
[6]Lead contact
*Correspondence: liujinping@znhospital.cn
https://doi.org/10.1016/j.isci.2023.108635

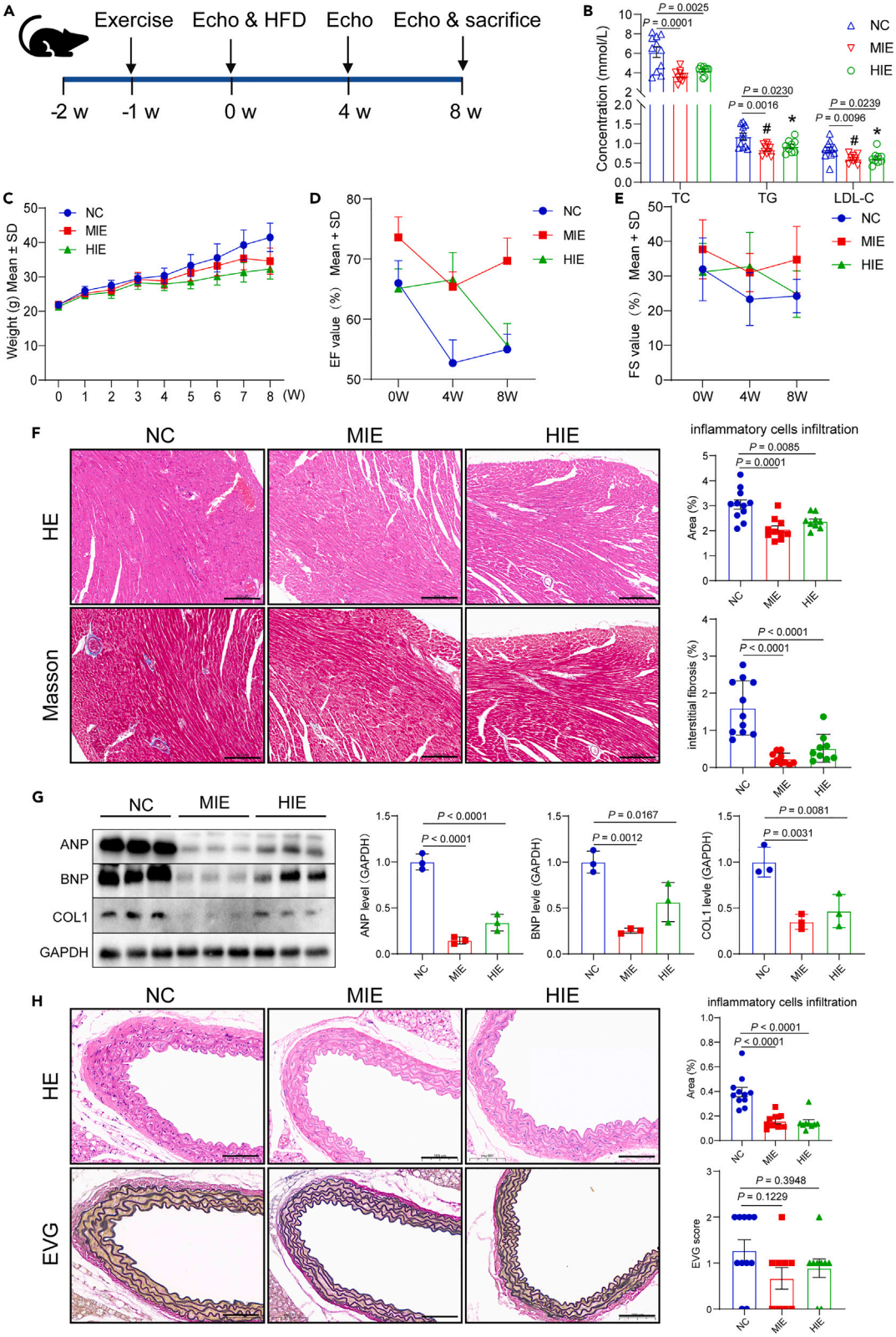
A
Exercise
Echo & HFD
Echo
Echo & sacrifice
-2 w
-1 w
0 w
4 w
8 w
B
Concentration (mmol/L)
NC
MIE
HIE
P = 0.0025
P = 0.0001
P = 0.0230
P = 0.0016
P = 0.0239
P = 0.0096
TC
TG
LDL-C
C
Weight (g) Mean ± SD
(W)
D
EF value (%) Mean + SD
0W
4W
8W
E
FS value (%) Mean + SD
F
HE
Masson
inflammatory cells infiltration
Area (%)
P = 0.0085
P = 0.0001
interstitial fibrosis (%)
P < 0.0001
P < 0.0001
G
ANP
BNP
COL1
GAPDH
ANP level (GAPDH)
BNP levle (GAPDH)
COL1 levle (GAPDH)
P = 0.0167
P = 0.0012
P = 0.0081
P = 0.0031
H
EVG
EVG score
P = 0.3948
P = 0.1229

Figure 1. The effect of physical exercise on high-fat diet fed mice

(A) Experimental design flowchart; (B) Serum lipid levels within each group (TC: F (DFn, DFd) = 12.44 (2, 27), p = 0.0001; TG: F (DFn, DFd) = 7.641 (2, 27), p = 0.0023; LDL-C: F (DFn, DFd) = 5.672 (2, 27), p = 0.0088; n = 11: 10: 9); (C) Body weights within each group (n = 11: 10: 9); (D) EF values within each group (n = 11: 10: 9); (E) FS values within each group (n = 11: 10: 9); (F) HE and Masson staining of mice hearts within each group (HE: F (DFn, DFd) = 11.50 (2, 27), p = 0.0002; Masson: F (DFn, DFd) = 22.26 (2, 27), p < 0.0001; n = 11: 10: 9), scale bar: 200 μm; (G) Western blotting results of ANP, BNP, and collagen 1 in each group (ANP: F (DFn, DFd) = 105.9 (2, 6), p < 0.0001; BNP: F (DFn, DFd) = 21.00 (2, 6), p = 0.0020; Col 1: F (DFn, DFd) = 16.43 (2, 6), p = 0.0037; n = 3: 3: 3); (H) HE and EVG staining of mice aortas within each group (HE: F (DFn, DFd) = 23.26 (2, 27), p < 0.0001; EVG: F (DFn, DFd) = 1.885 (2, 26), p = 0.1721; n = 11: 10: 9), scale bar: 100 μm. Data are presented as the mean ± SD.

investigate the relationship among various intensities of physical exercise, the spleen microbiome, and cardiac function, and attempted to investigate whether physical exercise could impact heart function by influencing the microbiome composition within the spleen.

RESULTS

The effect of exercise on HFD-fed mouse body weight, serum lipid levels, and cardiovascular function

Figure 1A represents the experimental design flowchart. All mice survived the 8-week training period except for one mouse in the HIE group, which died on Day 44. On Day 57, the serum lipid level of each mouse was measured. The results revealed that the high-fat diet (HFD) led to an increase in TC levels (NC group: 6.13 ± 1.82, MIE group: 3.68 ± 0.61, HIE group: 4.22 ± 0.44), TG levels (NC group: 1.18 ± 0.28, MIE group: 0.84 ± 0.13, HIE group: 0.93 ± 0.16) and LDL-C levels (NC group: 0.84 ± 0.23, MIE group: 0.60 ± 0.11, HIE group: 0.63 ± 0.16). However, different intensities of exercise significantly decreased the levels of TC, TG, and LDL-C compared with the NC group ($p < 0.05$, Figure 1B). Additionally, the mice in each group exhibited similar body weights prior to the experiment (NC group: 21.87 ± 0.77, MIE group: 21.93 ± 0.56, HIE group: 21.31 ± 0.57). After 1 week of training, a significant difference was observed between the NC group and HIE group (NC group: 25.99 ± 1.26 versus HIE group: 24.73 ± 1.08, $p < 0.05$). However, no significant difference was found between the NC group and MIE group (NC group: 25.99 ± 1.26 versus MIE group: 25.20 ± 0.93, $p > 0.05$) at this point (Figures 1C and S1A). Nonetheless, after seven weeks of training, a significant difference was found between the NC group and MIE group (NC group: 39.29 ± 4.39 versus MIE group: 35.36 ± 3.28, $p < 0.05$) (Figures 1C and S1A). Ejection fractions and fractional shortening were measured at 0 w, 4 w, and 8 w of exercise. No significant difference was observed within each group prior to exercise (EF values in the NC, MIE, and HIE groups: 65.98 ± 12.33, 73.59 ± 10.79, 65.08 ± 10.34, respectively) (FS values in the NC, MIE, and HIE groups: 31.97 ± 9.06, 37.71 ± 8.51, 31.19 ± 8.28, respectively) (Figures 1D and S1B). After 4 weeks of training, both the MIE group and the HIE group exhibited a significant difference in EF values compared with the NC group (NC group: 52.68 ± 12.81 versus MIE group: 65.39 ± 7.83, $p < 0.05$, NC group: 52.68 ± 12.81 versus HIE group: 66.57 ± 14.18, $p < 0.05$) (Figures 1D and S1B). At the conclusion of the training period, a significant difference in EF values was found between the MIE group and NC group (NC group: 54.95 ± 8.39 versus MIE group: 69.71 ± 11.92, $p < 0.05$, Figures 1D and S1B), whereas no significant difference in EF values was observed between the NC group and the HIE group (NC group: 54.95 ± 8.39 versus HIE group: 55.61 ± 10.93, $p > 0.05$, Figures 1D and S1B). In terms of the value of FS within each group, a significant difference was observed between the NC group and the HIE group after 4 weeks of training (NC group: 23.33 ± 7.59 versus HIE group: 32.70 ± 9.87, $p < 0.05$, Figures 1E and S1C), whereas no difference was found after 8 weeks of training (NC group: 24.22 ± 4.84 versus HIE group: 24.79 ± 6.69, $p > 0.05$, Figures 1E and S1C). Simultaneously, a significant difference was observed in the FS value between the NC group and MIE group after 8 weeks of training (NC group: 24.22 ± 4.84 versus MIE group: 34.75 ± 9.55, $p < 0.05$, Figures 1E and S1C), whereas no difference was found after 4 weeks of training (NC group: 23.33 ± 7.59 versus MIE group: 31.02 ± 5.48, $p > 0.05$, Figures 1E and S1C).

Exercise ameliorates pathological changes in the heart and aorta of mice fed a high-fat diet

Mouse hearts and aortas were collected after eight weeks of treadmill running and subjected to histological and immunohistochemical staining. Compared with the NC group, both the MIE group and HIE group exhibited a significant reduction in inflammatory cell infiltration and a decrease in the extent of interstitial fibrosis ($p < 0.05$, Figure 1F). Furthermore, we extracted mouse hearts to perform western blotting. We observed a significant reduction in the levels of ANP, BNP, and collagen 1 in both the MIE group and HIE group compared with the NC group ($p < 0.05$, Figure 1G). When comparing the effects of exercise on the mouse aorta, the results of HE staining revealed that the NC group exhibited a significantly higher infiltration of inflammatory cells than both the MIE group and HIE group ($p < 0.05$, Figure 1H). However, no significant difference was observed when comparing the NC group with either the MIE group or HIE group in terms of EVG scores ($p > 0.05$, Figure 1H).

The impact of exercise intervention on spleen alterations in high-fat diet (HFD)-fed mice

To assess the impact of exercise intervention on the spleens of mice fed an HFD, we collected spleen samples for histological and immunohistochemical staining, western blotting, and flow cytometry analysis. Histological and immunohistochemical staining revealed a significant increase in the infiltration of inflammatory cells, particularly macrophages, in the NC group when fed a HFD. However, various levels of exercise intervention resulted in a significant decrease in inflammatory cell infiltration and macrophages compared with the NC group ($p < 0.05$, Figure 2A). Additionally, we observed a significant reduction in the level of TNF-α in the spleens of both the MIE group and HIE group when compared with the NC group ($p < 0.05$, Figure 2A). Similarly, western blot analysis revealed a significant decrease in the level of TNF-α in the spleens of both the MIE group and HIE group when compared with the NC group ($p < 0.05$, Figure 2C). In the same way, both the MIE group

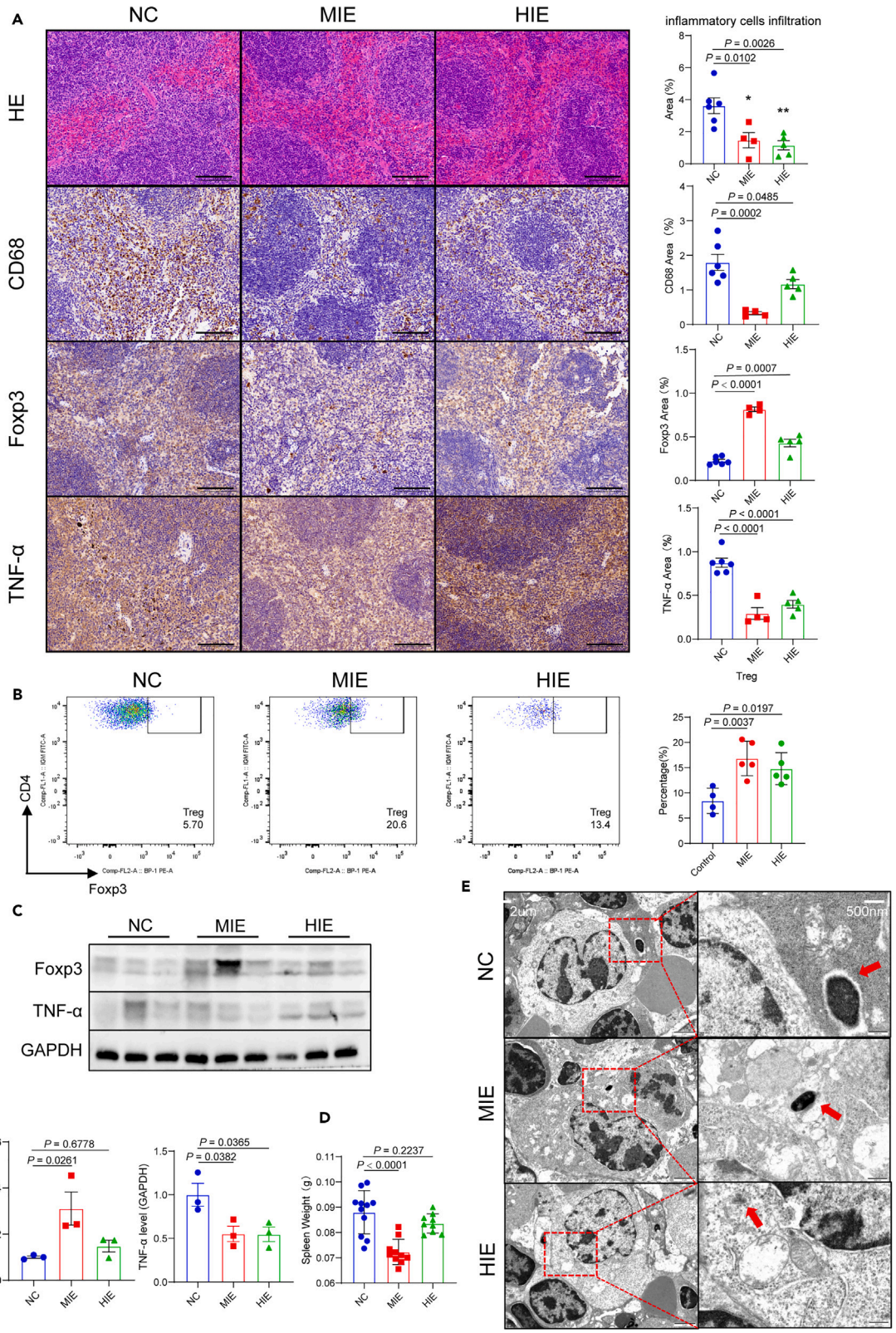
A
NC
MIE
HIE
HE
CD68
Foxp3
TNF-α
inflammatory cells infiltration
P = 0.0026
P = 0.0102
Area (%)
CD68 Area (%)
P = 0.0485
P = 0.0002
Foxp3 Area (%)
P = 0.0007
P < 0.0001
TNF-α Area (%)
P < 0.0001
P < 0.0001
B
CD4
Foxp3
Treg
5.70
Treg
20.6
Treg
13.4
Percentage(%)
P = 0.0197
P = 0.0037
Control
C
Foxp3
TNF-α
GAPDH
Foxp3 level (GAPDH)
P = 0.6778
P = 0.0261
TNF-α level (GAPDH)
P = 0.0365
P = 0.0382
D
Spleen Weight (g)
P = 0.2237
P < 0.0001
E
2μm
500nm

Figure 2. The impact of physical exercise on spleens of high-fat diet fed mice

(A) The results of HE, CD68, Foxp3, and TNF-α staining of mice spleens in each group (HE: F (DFn, DFd) = 10.19 (2, 12), p = 0.0026; CD68: F (DFn, DFd) = 15.46 (2, 12), p = 0.0005; Foxp3: F (DFn, DFd) = 90.54 (2, 12), p < 0.0001; TNF-α: F (DFn, DFd) = 34.36 (2, 12), p < 0.0001; n = 6: 4: 5), scale bar: 100 μm; (B) Treg cell levels in mice spleens within each group were measured by the Flow cytometer analysis (TNF-α: F (DFn, DFd) = 8.578 (2, 11), p = 0.0057; n = 4: 5: 5); (C) Western blotting results of Foxp3 and TNF-α in each group (Foxp3: F (DFn, DFd) = 6.297 (2, 6), p = 0.0336; TNF-α: F (DFn, DFd) = 6.379 (2, 6), p = 0.0327; n = 3: 3: 3); (D) Spleen weights within each group (TNF-α: F (DFn, DFd) = 17.01 (2, 27), p < 0.0001; n = 11: 10: 9); (E) the results of TEM examination in mice spleens within each group. Data are presented as the mean ± SD.

and the HIE group exhibited a decrease in mouse spleen weight compared with the NC group. Specifically, the spleen weight of the MIE group exhibited a significant reduction ($p < 0.05$, Figure 2D). However, there was a significant increase in the level of Treg cells in the spleens of both the MIE group and HIE group when compared with the NC group ($p < 0.05$, Figure 2A). Additionally, flow cytometry analysis demonstrated that the MIE group exhibited a significantly higher level of Treg cells in mouse spleens than the HIE group and NC group ($p < 0.05$, Figure 2B). Moreover, western blotting revealed a significant increase in the level of foxp3 in the spleens of the MIE group compared with the HIE group and NC group ($p < 0.05$, Figure 2C).

Exercise intervention alters spleen microbiome composition in the HFD-fed mice

Recently, Duan et al. reported that the microbiome of the spleen may play a role in the progression of an experimental autoimmune encephalomyelitis mouse model.[18] Interestingly, our TEM examination results revealed the presence of bacteria in the spleens of mice (Figure 2E). Consequently, we conducted 16S rRNA sequencing to investigate the alterations in the spleen microbiome among the NC, MIE, and HIE groups. First, the Venn diagram illustrated a significant decrease in the number of OTUs in the MIE group and HIE group compared with the NC group (Figure 3A). The taxonomic composition plots at the phylum level demonstrated that *Proteobacteria*, *Actinobacteria*, *Firmicutes*, and *Bacteroidetes* were the dominant bacterial communities in the spleens of the NC group, MIE group, and HIE group (Figure 3B). Moreover, the dominant phylum observed in the spleen microbiome of mice from all groups was *Proteobacteria* (Figures 3G and 3H). Additionally, we discovered a significant increase in the abundance of *L. johnsonii* at the species level in both the MIE group and HIE group compared with the NC group (Figures 3C and 3D). Interestingly, a correlation analysis revealed a positive association between the abundance of *Lactobacillus johnsonii* and Treg cells in the spleens of mice ($R^2 = 0.8616$, Figure 3E). Antibiotic-treated mice fed *L. johnsonii* exhibited a significant increase in spleen Treg cells compared with the control group ($p < 0.05$, Figure 3F). However, no significant difference was found when comparing the inactive Lacto group with the control group ($p > 0.05$, Figure 3F). These results suggest that *Lactobacillus johnsonii* may contribute to the production of Treg cells.

Next, we used a Chao 1 estimator, the Shannon diversity index, and drew a rank-abundance curve to assess the richness and diversity of the spleen microbiota (Figures 4A–4C). Although no significant differences were observed in either the Chao 1 estimator or Shannon diversity index, we found that the NC group exhibited lower richness than the MIE group and HIE group, whereas the MIE group exhibited lower diversity than the NC group and HIE group. Furthermore, we employed PCoA analysis to evaluate beta diversity (Figure 4D), and ANOSIM analysis indicated that the differences between groups were more pronounced than the differences within groups (NC to MIE, $R = 0.11$, $p = 0.007$; NC to HIE, $R = 0.096$, $p = 0.032$, Figure 4E). These findings suggest that the protective effects of physical exercise may be mediated through the spleen microbiome.

Species differences and marker species analysis in each group

To identify the key species responsible for these differences, we constructed a species composition heatmap and utilized linear discriminant analysis effect size (LEfSe) and random forest analysis. These analyses allowed us to determine the species that played a primary role in shaping the dissimilarities among the groups and aided in filtering out the most significant species within each group. The species composition heatmap revealed that the NC group was enriched in *Bifidobacterium pseudolongum, Hymenobacter* sp., *Pseudonocardia* sp., *Nocardioides marinquilinus, Nocardioides lentus, Spirosoma pomorum, Rhodococcus corynebacterioides,* and *Geodermatophilus* sp. (Figures 5A and 5B). Conversely, the MIE group exhibited enrichment in *Lactobacillus delbrueckii, Akkermansia muciniphila,* and *Pseudomonas rhizosphaerae*, whereas the HIE group exhibited enrichment in *Ralstonia insidiosa, L. johnsonii, Lactobacillus reuteri, Lactobacillus salivarius, Corynebacterium pyruviciproducens, Acinetobacter venetianus, Lachnospiraceae bacterium*, and *Bacteroides vulgatus* (Figures 5A and 5B). Moreover, the random forest analysis emphasized the importance of *B. pseudolongum* in the NC group, *Akkermansia muciniphila* in the MIE group, and *Lactobacillus johnsonii* in the HIE group (Figure 5C). Similarly, the LEfSe analysis also highlighted the significance of *B. pseudolongum* in the NC group and *L. johnsonii* in the HIE group, with *Acinetobacter harbinensis* being prominent in the MIE group (Figures 5D and 5E).

We utilized PICRUSt2 (phylogenetic investigation of communities by reconstruction of unobserved states) to predict the potential roles of the spleen microbiome. The findings revealed that the dominant function of the spleen microbiota was biosynthesis, particularly in amino acid biosynthesis, cofactors, prosthetic groups, electron carriers, and vitamin biosynthesis, as well as nucleoside and nucleotide biosynthesis (Figure 6). In addition, the spleen microbiome demonstrated other functions, such as degradation/utilization/assimilation, detoxification, generation of precursor metabolites and energy, glycan pathways, macromolecule modification, and metabolic clusters (Figure 6).

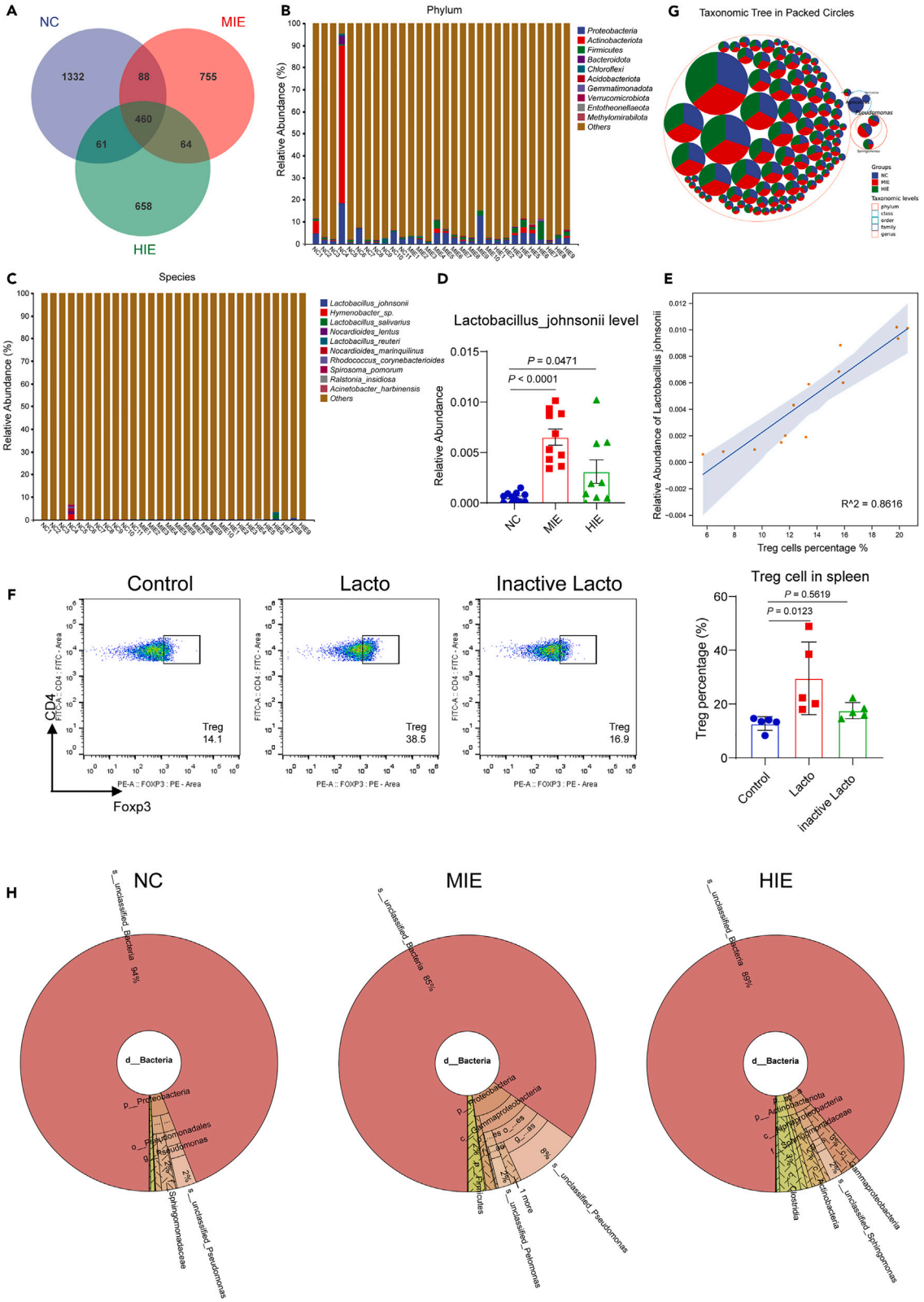
A
NC
MIE
HIE
1332
88
755
460
61
64
658
B
Phylum
Relative Abundance (%)
Proteobacteria
Actinobacteriota
Firmicutes
Bacteroidota
Chloroflexi
Acidobacteriota
Gemmatimonadota
Verrucomicrobiota
Entotheonellaeota
Methylomirabilota
Others
G
Taxonomic Tree in Packed Circles
Pseudomonas
Groups
NC
MIE
HIE
Taxonomic levels
phylum
class
order
family
genus
C
Species
Relative Abundance (%)
Lactobacillus_johnsonii
Hymenobacter_sp.
Lactobacillus_salivarius
Nocardioides_lentus
Lactobacillus_reuteri
Nocardioides_marinquilinus
Rhodococcus_corynebacterioides
Spirosoma_pomorum
Ralstonia_insidiosa
Acinetobacter_harbinensis
Others
D
Lactobacillus_johnsonii level
Relative Abundance
P = 0.0471
P < 0.0001
NC
MIE
HIE
E
Relative Abundance of Lactobacillus johnsonii
R^2 = 0.8616
Treg cells percentage %
F
Control
Lacto
Inactive Lacto
CD4
Foxp3
Treg
14.1
38.5
16.9
PE-A :: FOXP3 : PE - Area
FITC-A :: CD4 : FITC - Area
Treg cell in spleen
Treg percentage (%)
P = 0.5619
P = 0.0123
Control
Lacto
inactive Lacto
H
NC
MIE
HIE
s__unclassified_Bacteria 94%
s__unclassified_Bacteria 85%
s__unclassified_Bacteria 89%
d__Bacteria
p__Proteobacteria
o__Pseudomonadales
g__Pseudomonas
Sphingomonadaceae
s__unclassified_Pseudomonas
p__Actinobacteriota
Alphaproteobacteria
Gammaproteobacteria
Clostridia
s__unclassified_Sphingomonas

Figure 3. 16S rRNA sequencing revealed alterations in the spleen microbiota in each group

(A) Venn plot; (B) phylum level; (C) species level; (D) relative abundance of Lactobacillus johnsonii in each group (F (DFn, DFd) = 16.08 (2, 27), p < 0.0001; n = 11: 10: 9); (E) correlation ship between Lactobacillus johnsonii and Treg cells (R^2 = 0.8616); (F) Treg cell levels in the mouse spleens within each group were measured by the flow cytometry analysis (Treg: F (DFn, DFd) = 5.684 (2, 12), p = 0.0183; n = 5: 5: 5); (G) taxonomic tree in packed circles; (H) Krona analysis of the bacterial community structures of each group. Data are presented as the mean ± SD, n = 11: 10: 9.

DISCUSSION

Consumption of a HFD has been shown to be an independent risk factor for human health,[19] potentially contributing to various diseases, such as obesity,[20] cardiovascular diseases,[21] and immune system imbalance.[22] As indicated above, the echocardiographic analysis revealed a decrease in the left ventricular ejection fraction and fractional shortening when mice were fed a HFD. These findings are consistent with the study conducted by Ge et al., where they observed a decrease in EF and FS values in mice following HFD intake.[23] Moreover, the consumption of a HFD also induces an augmented infiltration of inflammatory cells (such as macrophages), along with an enhanced secretion of inflammatory cytokines (such as TNF-α). Conversely, there is a decrease in Treg cell infiltration within the spleens of mice, indicating that HFD intake disrupts the balance between inflammation and anti-inflammation in this organ. TNF-α has been validated as a marker for monitoring the dynamic fluctuations in inflammation in response to high-fat meals and exercise.[24] In the present study, we have demonstrated that various intensities of exercise can mitigate the detrimental effects of a HFD and prevent abnormal damage to the hearts and aortas of mice. Physical exercise has been proven to be beneficial for cardiac function,[3,4] particularly when conducted as a moderate intensity exercise. Xiao et al. discovered that moderate exercise plays a protective role against myocardial infarction.[25] However, in our study, the HIE group exhibited impaired cardiac function in mice. Richard et al. conducted a study to assess the effects of high-intensity exercise on left ventricular systolic and diastolic function.[26] The results revealed a decrease in LVEF in the high-intensity exercise group compared with the normal group. Similarly, Darren and his colleagues also observed damage to LVEF during high-intensity exercise.[27] The potential mechanism underlying impaired cardiac function following strenuous exercise is that high-intensity exercise induces significant physiological stress, which affects the secretion of catecholamines. Sustained elevations in catecholamines are believed to desensitize cardiac beta receptors, resulting in impaired cardiac function.[28] Therefore, moderate-intensity exercise is encouraged as a daily practice rather than high-intensity exercise.

Furthermore, physical exercise resulted in alterations in the composition of the spleen microbiome, suggesting that the microbiome of the spleen may play a vital role in the protective effects of physical exercise. Based on the findings of the Human Microbiome Project (HMP),[29] it is well established that a vast array of commensal (nonpathogenic) and pathogenic microbial species reside in the human body, having co-evolved with the human genome, adaptive immune system, and diet. In recent years, the tissue microbiota has gained recognition for its role in maintaining homeostasis, thereby emerging as a promising therapeutic target for numerous diseases.[30] As mentioned earlier, Duan et al. observed an enrichment of *Enterobacter* in the spleens of the EAE group. Furthermore, they found that oral administration of live *Enterobacter* sp. significantly accelerated the clinical scores of EAE mice.[18] In our study, we discovered alterations in the spleen microbiome of mice following different intensity exercises. The species composition map revealed a significant enrichment of *Lactobacillus*

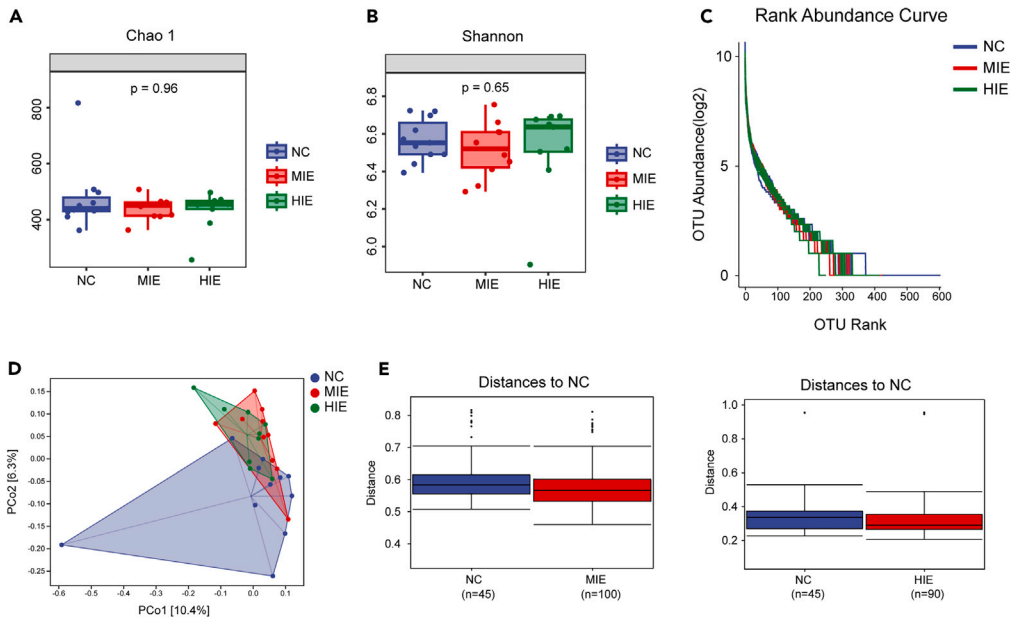

Figure 4. Alpha and beta diversities of the microbiota

(A) Chao1 estimator; (B) Shannon diversity index; (C) rank-abundance curve; (D) PCoA analysis; (E) ANOSIM analysis, NC to MIE, R = 0.11, p = 0.007; NC to HIE, R = 0.096, p = 0.032, n = 11: 10: 9.

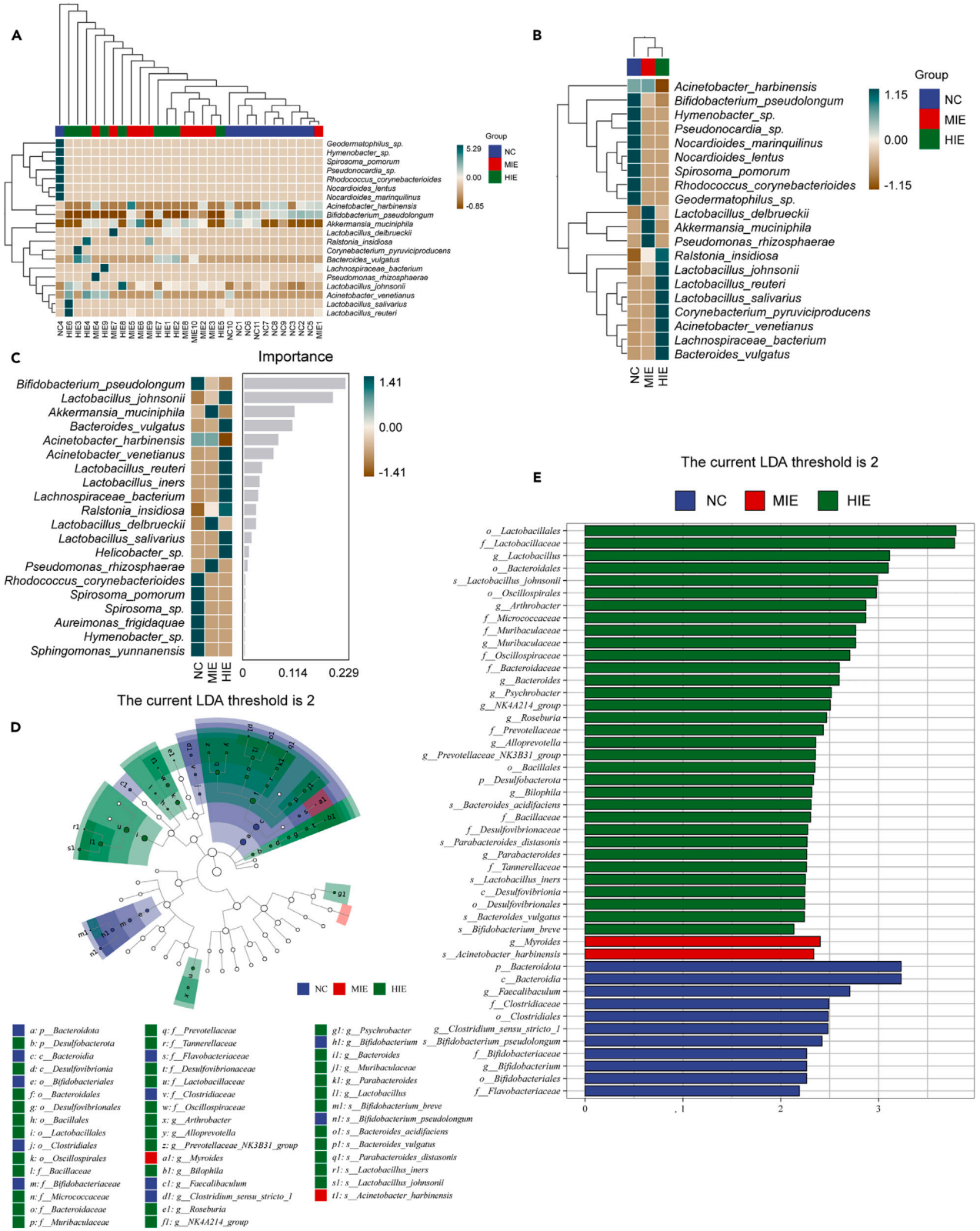

Figure 5. Species differences and marker species analysis

(A) Species composition heatmap in each mouse; (B) Species composition heatmap in each group; (C) Random Forest analysis to identify the important species in each group; (D and E) LEfSe analysis, n = 11: 10: 9.

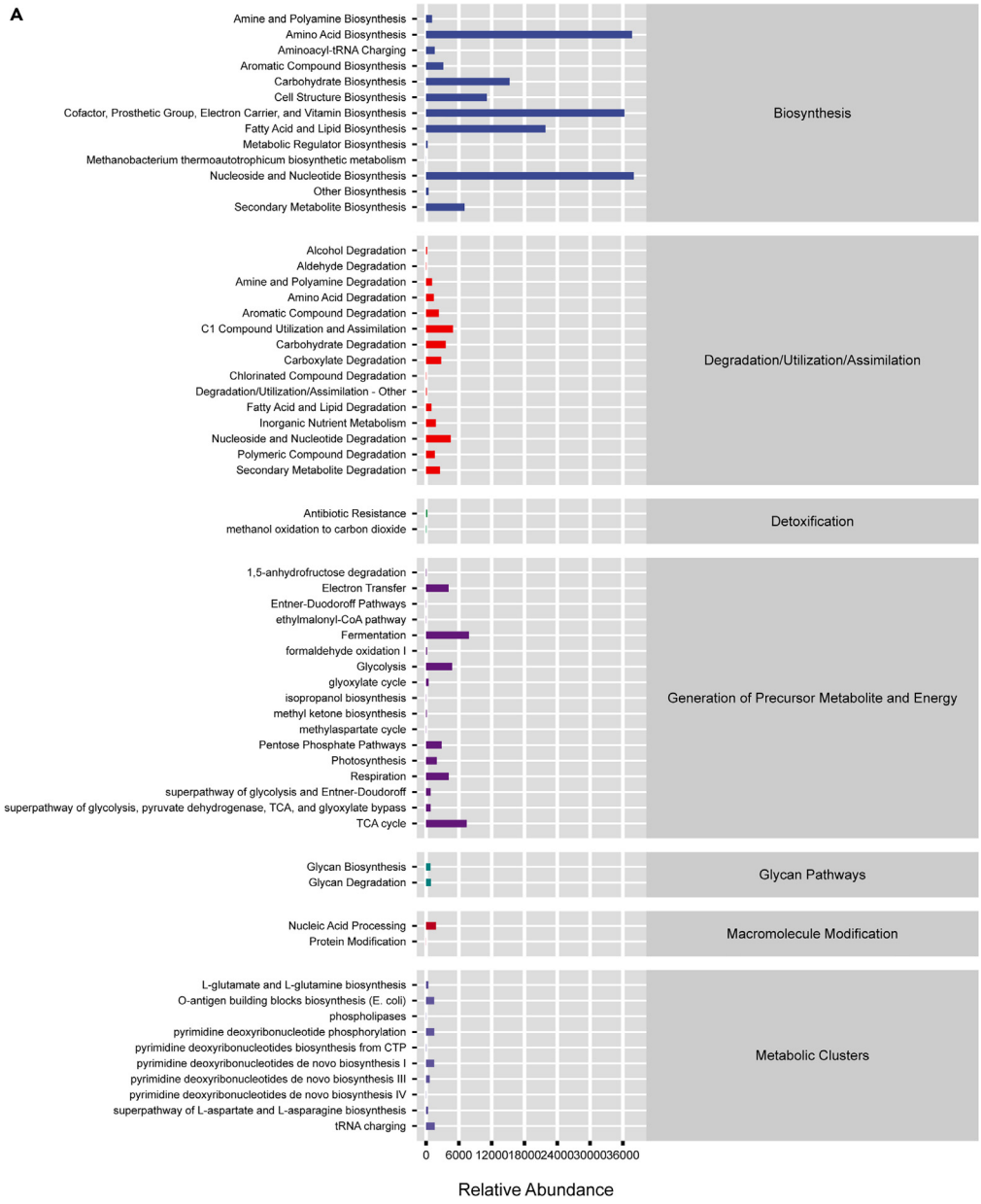

Figure 6. PICRUSt2 analysis to predict the potential role of the spleen microbiome and spleen microbiota participating in biosynthesis pathways

johnsonii in both the MIE group and HIE group compared with the NC group. *Lactobacillus johnsonii* (*L. johnsonii*) has been identified as a beneficial bacterium belonging to the *Lactobacillus* genus. Current research has demonstrated the potential of *L. johnsonii* in enhancing memory function through the brain-gut axis and its role in regulating metabolic-related disorders.[31] Additionally, it has been demonstrated that *L. johnsonii* stimulates the STAT3 pathway, enhances CD206+ macrophage activation, and increases the secretion of IL-10.[31] Furthermore, Luo et al. revealed that supplementation with *L. johnsonii* can ameliorate renal dysfunction and improve survival in mice with experimental lupus nephritis. Moreover, *L. johnsonii* has the ability to shift the Treg-Th17 balance in favor of Treg cells.[32] These findings emphasize the anti-inflammatory role of *L. johnsonii* in maintaining human homeostasis. In our study, we observed a positive correlation between the level of *L. johnsonii* and the level of Treg cells in the spleens of mice, antibiotic-treated mice supplemented *Lactobacillus johnsonii* exhibited a significant increase in spleen Treg cells compared with the control group. Several studies have examined the impact of physical exercise on Treg cell production and have reached varying conclusions regarding the underlying mechanisms.[33,34] Therefore, further investigations are needed to clarify whether the potential mechanism by which physical exercise affects Treg cell production is mediated through *L. johnsonii*. This will be the focus of our future studies.

LEfSe analysis and random forest analysis were utilized to identify the primary species responsible for these differences and to pinpoint the key species within each group. The results unequivocally showcased the significant roles of *B. pseudolongum* in the NC group, *Akkermansia muciniphila* in the MIE group, and *L. johnsonii* in the HIE group. *B. pseudolongum*, a member of the Actinobacteria phylum, is consistently recognized as a beneficial bacterium involved in maintaining host homeostasis. A recent study reported that the acetate produced by *B. pseudolongum* can inhibit the proliferation of hepatocellular carcinoma associated with nonalcoholic fatty liver disease and induce apoptosis in tumor cells.[35] However, it should be noted that *B. pseudolongum* may exhibit a bidirectional role in host metabolism. Weaver et al.[36] demonstrated that *B. pseudolongum* was highly expressed in the offspring of mice fed an HFD. This observation suggests that various strains of *B. pseudolongum* may have different metabolic effects, potentially explaining its dual impact on host metabolism. Marco et al.[37] conducted a phylogenomic analysis of the genome sequences of 60 *B. pseudolongum* strains, suggesting that the *B. pseudolongum* species is composed of two subspecies: *B. pseudolongum* subsp. *globosum* and *B. pseudolongum* subsp. *pseudolongum*. It is plausible that these subspecies may play distinct roles in maintaining host homeostasis. In our study, we observed an increase in the abundance of *B. pseudolongum* in the NC group. Therefore, further investigations are warranted to identify the specific subspecies of *B. pseudolongum* and elucidate their respective roles in the spleen of mice fed a HFD in future studies. *A. muciniphila*, first documented in 2004, has been extensively studied to explore its potential role in humans.[38] Previous research has highlighted *A. muciniphila* as a promising candidate for the treatment of microbiota-related disorders, such as colitis, metabolic syndrome, and immune diseases.[39] However, further studies are needed to elucidate the role of *A. muciniphila* in the spleen. Additionally, PICRUSt2 analysis indicated that the main function of the spleen microbiome is biosynthesis, suggesting that the microbes may influence the immune microenvironment of the spleen through biosynthesis pathways.

Sample contamination is a major concern in tissue microbiome sequencing. Contaminant DNA can originate from various sources, such as the sampling and laboratory environments, researchers themselves, plastic consumables, nucleic acid extraction kits, laboratory reagents (including PCR mastermixes), and cross-contamination from other samples and sequencing runs.[40] Therefore, in our study, all sample collections were meticulously conducted in a clean bench environment to mitigate the risk of contamination.

In conclusion, our study revealed the impact of moderate-intensity exercise on the composition of the spleen microbiome in mice and demonstrated reduced risks of cardiovascular diseases in HFD-fed mice. Additionally, we identified the significant roles of *B. pseudolongum* in the NC group, *A. muciniphila* in the MIE group, and *Lactobacillus johnsonii* in the HIE group, respectively.

Limitations of the study

In this study, we discovered the impact of moderate-intensity exercise on the spleen microbiome composition in mice and reduced risks of cardiovascular diseases in HFD-fed mice. Furthermore, we observed that the abundance of *L. johnsonii* in the spleen influenced the production of Treg cells. However, the potential mechanism by which *L. johnsonii* promotes Treg cell production remains to be validated in future studies.

STAR★METHODS

Detailed methods are provided in the online version of this paper and include the following:

- KEY RESOURCES TABLE
- RESOURCE AVAILABILITY
  - Lead contact
  - Materials availability
  - Data and code availability
- EXPERIMENTAL MODEL AND STUDY PARTICIPANT DETAILS
  - Animals and protocols
  - Microbiota transplantation
  - 16S rRNA sequence
- METHOD DETAILS
  - Measurement of TC, TG, and LDL-C
  - Transmission electron microscopy (TEM) analysis
  - Histological and immunohistochemical staining
  - Western blotting
  - Flow cytometry analysis
- QUANTIFICATION AND STATISTICAL ANALYSIS

SUPPLEMENTAL INFORMATION

Supplemental information can be found online at https://doi.org/10.1016/j.isci.2023.108635.

ACKNOWLEDGMENTS

The authors thank the excellent assistance of Weina Guo and Xing Chen during the study. This work was financially supported by the National Natural Science Foundation of China (81974039), Key Research and Development Project of Hubei Provincial Department of Science and Technology (2020BCB053), and Talent Project of Zhongnan Hospital of Hubei Province (20200201).

AUTHOR CONTRIBUTIONS

J.X. and W.G. designed and performed the experiments, analyzed the data, and wrote the manuscript. J.L. reviewed the manuscript. X.C. designed the experiment. Y.L. analyzed the data. All authors contributed to the article and approved the submitted version.

DECLARATION OF INTERESTS

The author declares no conflict of interest.

Received: August 27, 2023
Revised: November 15, 2023
Accepted: December 1, 2023
Published: December 5, 2023

REFERENCES

1. Tsao, C.W., Aday, A.W., Almarzooq, Z.I., Alonso, A., Beaton, A.Z., Bittencourt, M.S., Boehme, A.K., Buxton, A.E., Carson, A.P., Commodore-Mensah, Y., et al. (2022). Heart Disease and Stroke Statistics-2022 Update: A Report From the American Heart Association. Circulation *145*, e153–e639.
2. Hu, S.S. (2023). Report on cardiovascular health and diseases in China 2021: an updated summary. J. Geriatr. Cardiol. *20*, 399–430.
3. Patnode, C.D., Redmond, N., Iacocca, M.O., and Henninger, M. (2022). Behavioral Counseling Interventions to Promote a Healthy Diet and Physical Activity for Cardiovascular Disease Prevention in Adults Without Known Cardiovascular Disease Risk Factors: Updated Evidence Report and Systematic Review for the US Preventive Services Task Force. JAMA *328*, 375–388.
4. Artinian, N.T., Fletcher, G.F., Mozaffarian, D., Kris-Etherton, P., Van Horn, L., Lichtenstein, A.H., Kumanyika, S., Kraus, W.E., Fleg, J.L., Redeker, N.S., et al. (2010). Interventions to promote physical activity and dietary lifestyle changes for cardiovascular risk factor reduction in adults: a scientific statement from the American Heart Association. Circulation *122*, 406–441.
5. Chen, H., Chen, C., Spanos, M., Li, G., Lu, R., Bei, Y., and Xiao, J. (2022). Exercise training maintains cardiovascular health: signaling pathways involved and potential therapeutics. Signal Transduct. Target. Ther. *7*, 306.
6. Valenzuela, P.L., Ruilope, L.M., Santos-Lozano, A., Wilhelm, M., Kränkel, N., Fiuza-Luces, C., and Lucia, A. (2023). Exercise benefits in cardiovascular diseases: from mechanisms to clinical implementation. Eur. Heart J. *44*, 1874–1889.
7. Lori, A., Perrotta, M., Lembo, G., and Carnevale, D. (2017). The Spleen: A Hub Connecting Nervous and Immune Systems in Cardiovascular and Metabolic Diseases. Int. J. Mol. Sci. *18*, 1216.
8. Carnevale, D., Pallante, F., Fardella, V., Fardella, S., Iacobucci, R., Federici, M., Cifelli, G., De Lucia, M., and Lembo, G. (2014). The angiogenic factor PlGF mediates a neuroimmune interaction in the spleen to allow the onset of hypertension. Immunity *41*, 737–752.
9. Mellak, S., Ait-Oufella, H., Esposito, B., Loyer, X., Poirier, M., Tedder, T.F., Tedgui, A., Mallat, Z., and Potteaux, S. (2015). Angiotensin II mobilizes spleen monocytes to promote the development of abdominal aortic aneurysm in Apoe-/- mice. Arterioscler. Thromb. Vasc. Biol. *35*, 378–388.
10. Feng, L., Huang, F., Ma, Y., and Tang, J. (2021). The Effect of High-Fat Diet and Exercise Intervention on the TNF-alpha Level in Rat Spleen. Front. Immunol. *12*, 671167.
11. Massier, L., Chakaroun, R., Tabei, S., Crane, A., Didt, K.D., Fallmann, J., von Bergen, M., Haange, S.B., Heyne, H., Stumvoll, M., et al. (2020). Adipose tissue derived bacteria are associated with inflammation in obesity and type 2 diabetes. Gut *69*, 1796–1806.
12. Liu, X.Y., Li, J., Zhang, Y., Fan, L., Xia, Y., Wu, Y., Chen, J., Zhao, X., Gao, Q., Xu, B., et al. (2022). Kidney microbiota dysbiosis contributes to the development of hypertension. Gut Microb. *14*, 2143220.
13. Suppli, M.P., Bagger, J.I., Lelouvier, B., Broha, A., Demant, M., Kønig, M.J., Strandberg, C., Lund, A., Vilsbøll, T., and Knop, F.K. (2021). Hepatic microbiome in healthy lean and obese humans. JHEP Rep. *3*, 100299.
14. Dominy, S.S., Lynch, C., Ermini, F., Benedyk, M., Marczyk, A., Konradi, A., Nguyen, M., Haditsch, U., Raha, D., Griffin, C., et al. (2019). Porphyromonas gingivalis in Alzheimer's disease brains: Evidence for disease causation and treatment with small-molecule inhibitors. Sci. Adv. *5*, eaau3333.
15. Nejman, D., Livyatan, I., Fuks, G., Gavert, N., Zwang, Y., Geller, L.T., Rotter-Maskowitz, A., Weiser, R., Mallel, G., Gigi, E., et al. (2020). The human tumor microbiome is composed of tumor type-specific intracellular bacteria. Science *368*, 973–980.
16. Deng, Y., Ge, X., Li, Y., Zou, B., Wen, X., Chen, W., Lu, L., Zhang, M., Zhang, X., Li, C., et al. (2021). Identification of an intraocular microbiota. Cell Discov. *7*, 13.
17. Zhou, L.J., Lin, W.Z., Meng, X.Q., Zhu, H., Liu, T., Du, L.J., Bai, X.B., Chen, B.Y., Liu, Y., Xu, Y., et al. (2023). Periodontitis exacerbates atherosclerosis through Fusobacterium nucleatum-promoted hepatic glycolysis and lipogenesis. Cardiovasc. Res. *119*, 1706–1717.
18. Zhou, L.J., Lin, W.Z., Liu, T., Chen, B.Y., Meng, X.Q., Li, Y.L., Du, L.J., Liu, Y., Qian, Y.C., Zhu, Y.Q., and Duan, S.Z. (2023). Oral Pathobionts Promote MS-like Symptoms in Mice. J. Dent. Res. *102*, 217–226.
19. Frazier, K., Kambal, A., Zale, E.A., Pierre, J.F., Hubert, N., Miyoshi, S., Miyoshi, J., Ringus, D.L., Harris, D., Yang, K., et al. (2022). High-fat diet disrupts REG3gamma and gut microbial rhythms promoting metabolic dysfunction. Cell Host Microbe *30*, 809–823.e6.
20. Maes, B., Fayazpour, F., Catrysse, L., Lornet, G., Van De Velde, E., De Wolf, C., De Prijck, S., Van Moorleghem, J., Vanheerswynghels, M., Deswarte, K., et al. (2023). STE20 kinase TAOK3 regulates type 2 immunity and metabolism in obesity. J. Exp. Med. *220*, e20210788.
21. Wu, Q., Gao, Z.J., Yu, X., and Wang, P. (2022). Dietary regulation in health and disease. Signal Transduct. Target. Ther. *7*, 252.
22. Beyaz, S., Chung, C., Mou, H., Bauer-Rowe, K.E., Xifaras, M.E., Ergin, I., Dohnalova, L., Biton, M., Shekhar, K., Eskiocak, O., et al. (2021). Dietary suppression of MHC class II expression in intestinal epithelial cells enhances intestinal tumorigenesis. Cell Stem Cell *28*, 1922–1935.e5.
23. Xu, H., Yu, W., Sun, M., Bi, Y., Wu, N.N., Zhou, Y., Yang, Q., Zhang, M., Ge, J., Zhang, Y., and Ren, J. (2023). Syntaxin17 contributes to obesity cardiomyopathy through promoting mitochondrial Ca(2+) overload in a Parkin-MCUb-dependent manner. Metabolism *143*, 155551.
24. Calder, P.C., Ahluwalia, N., Albers, R., Bosco, N., Bourdet-Sicard, R., Haller, D., Holgate, S.T., Jönsson, L.S., Latulippe, M.E., Marcos, A., et al. (2013). A consideration of biomarkers to be used for evaluation of inflammation in human nutritional studies. Br. J. Nutr. *109*, S1–S34.
25. Zhou, Q., Deng, J., Pan, X., Meng, D., Zhu, Y., Bai, Y., Shi, C., Duan, Y., Wang, T., Li, X., et al. (2022). Gut microbiome mediates the protective effects of exercise after myocardial infarction. Microbiome *10*, 82.
26. Scott, J.M., Esch, B.T., Haykowsky, M.J., Paterson, I., Warburton, D.E.R., Chow, K.,

Cheng Baron, J., Lopaschuk, G.D., and Thompson, R.B. (2010). Effects of high intensity exercise on biventricular function assessed by cardiac magnetic resonance imaging in endurance trained and normally active individuals. Am. J. Cardiol. *106*, 278–283.

27. Cote, A.T., Bredin, S.S.D., Phillips, A.A., Koehle, M.S., Glier, M.B., Devlin, A.M., and Warburton, D.E.R. (2013). Left ventricular mechanics and arterial-ventricular coupling following high-intensity interval exercise. J. Appl. Physiol. *115*, 1705–1713.
28. Banks, L., Sasson, Z., Busato, M., and Goodman, J.M. (2010). Impaired left and right ventricular function following prolonged exercise in young athletes: influence of exercise intensity and responses to dobutamine stress. J. Appl. Physiol. *108*, 112–119.
29. Human Microbiome Project Consortium (2012). A framework for human microbiome research. Nature *486*, 215–221.
30. Zhao, K., and Hu, Y. (2020). Microbiome harbored within tumors: a new chance to revisit our understanding of cancer pathogenesis and treatment. Signal Transduct. Target. Ther. *5*, 136.
31. Jia, D.J.C., Wang, Q.W., Hu, Y.Y., He, J.M., Ge, Q.W., Qi, Y.D., Chen, L.Y., Zhang, Y., Fan, L.N., Lin, Y.F., et al. (2022). Lactobacillus johnsonii alleviates colitis by TLR1/2-STAT3 mediated CD206(+) macrophages(IL-10) activation. Gut Microb. *14*, 2145843.
32. Mu, Q., Zhang, H., Liao, X., Lin, K., Liu, H., Edwards, M.R., Ahmed, S.A., Yuan, R., Li, L., Cecere, T.E., et al. (2017). Control of lupus nephritis by changes of gut microbiota. Microbiome *5*, 73.
33. Proschinger, S., Winker, M., Joisten, N., Bloch, W., Palmowski, J., and Zimmer, P. (2021). The effect of exercise on regulatory T cells: A systematic review of human and animal studies with future perspectives and methodological recommendations. Exerc. Immunol. Rev. *27*, 142–166.
34. Proschinger, S., Schenk, A., Weßels, I., Donath, L., Rappelt, L., Metcalfe, A.J., and Zimmer, P. (2023). Intensity- and time-matched acute interval and continuous endurance exercise similarly induce an anti-inflammatory environment in recreationally active runners: focus on PD-1 expression in T(regs) and the IL-6/IL-10 axis. Eur. J. Appl. Physiol. *123*, 2575–2584.
35. Song, Q., Zhang, X., Liu, W., Wei, H., Liang, W., Zhou, Y., Ding, Y., Ji, F., Ho-Kwan Cheung, A., Wong, N., and Yu, J. (2023). Bifidobacterium pseudolongum-generated acetate suppresses non-alcoholic fatty liver disease-associated hepatocellular carcinoma. J. Hepatol. *79*, 1352–1365.
36. Korgan, A.C., Foxx, C.L., Hashmi, H., Sago, S.A., Stamper, C.E., Heinze, J.D., O'Leary, E., King, J.L., Perrot, T.S., Lowry, C.A., and Weaver, I.C.G. (2022). Effects of paternal high-fat diet and maternal rearing environment on the gut microbiota and behavior. Sci. Rep. *12*, 10179.
37. Lugli, G.A., Duranti, S., Albert, K., Mancabelli, L., Napoli, S., Viappiani, A., Anzalone, R., Longhi, G., Milani, C., Turroni, F., et al. (2019). Unveiling Genomic Diversity among Members of the Species Bifidobacterium pseudolongum, a Widely Distributed Gut Commensal of the Animal Kingdom. Appl. Environ. Microbiol. *85*, e03065-18.
38. Hagi, T., and Belzer, C. (2021). The interaction of Akkermansia muciniphila with host-derived substances, bacteria and diets. Appl. Microbiol. Biotechnol. *105*, 4833–4841.
39. Zhou, K. (2017). Akkermansia muciniphilaStrategies to promote abundance of , an emerging probiotics in the gut, evidence from dietary intervention studies. J. Funct.Foods *33*, 194–201.
40. Eisenhofer, R., Minich, J.J., Marotz, C., Cooper, A., Knight, R., and Weyrich, L.S. (2019). Contamination in Low Microbial Biomass Microbiome Studies: Issues and Recommendations. Trends Microbiol. *27*, 105–117.

STAR★METHODS

KEY RESOURCES TABLE

REAGENT or RESOURCE	SOURCE	IDENTIFIER
Antibodies		
Rabbit anti-COLA1	Cell Signaling Technology	Cat# 72026S; RRID: AB_2904565
Rabbit anti-ANP	Absin	Cat# 123943;
Rabbit anti-BNP	ABclonal	Cat# A2179;
Rabbit anti-Foxp3	ABclonal	Cat# A4953; RRID: AB_2863396
Rabbit anti-TNF-α	ABclonal	Cat# A0277
Rabbit anti-GAPDH	Cell Signaling Technology	Cat# 5174;
Bacterial and virus strains		
Lactobacillus johnsonii (DSM 10533)	Mingzhou Biotechnology Co., Ltd., China	Cat# BMZ133557
Chemicals, peptides, and recombinant proteins		
Vancomycin	BioFroxx	Cat#: 1161GR001
neomycin sulphate	Solarbio	Cat#: N8090
metronidazole	Solarbio	Cat#: M8060
Ampicillin	Solarbio	Cat#: A8180
Deposited data		
Raw 16S rRNA data	This paper	SRA: PRJNA1029919
Experimental models: Organisms/strains		
Mouse: C57BL/6J	Wuhan Shulaibao Biotechnology Co., Ltd., China	N/A
Oligonucleotides		
16S rRNA V3-V4 region primers, forwards primer: ACTCCTACGGGAGGCAGCA, reverse primer: GGACTACHVGGGTWTCTAAT	This paper	N/A
Software and algorithms		
QIIME2 (version 2019.4)	This paper	https://qiime2.org
R version 4.0.2	R package	https://www.r-project.org/
GraphPad Prism 9	GraphPad Software	https://www.graphpad.com/scientific-software/prism/
ImageJ	NIH	https://ImageJ.nih.gov/ij/
FlowJo software	FlowJo, Ashland, OR, USA	https://www.flowjo.com/solutions/flowjo
Genescloud	This paper	https://www.genescloud.cn/chart/chartOverview
Other		
small animal treadmill	Science Biotechnology, Jiangsu, China	Cat#: SA101
ultrasonic cardiogram	VINNO, Jiangsu, China	Cat#: D6 LAB
flow cytometer	BD Fortessa; BD Biosciences, San Jose, CA, USA	Cat#: FACSCanto II

RESOURCE AVAILABILITY

Lead contact

Further information and requests for resources should be directed to and will be fulfilled by the lead contact, Jinping Liu (liujinping@znhospital.cn).

Materials availability

This study did not generate new unique reagents.

Data and code availability

- The raw 16s RNA-seq data generated in this study is available on SRA under the accession code: PRJNA1029919. The names of the repository/repositories and accession number(s) can be found below: https://www.ncbi.nlm.nih.gov/bioproject/PRJNA1029919.
- The data utilized to support the findings of this study can be obtained from the corresponding author upon request.
- The code used to call ASVs, assign taxonomic annotations, perform the analysis, and create figures is available at https://www.genescloud.cn/chart/chartOverview.
- Any additional information required to reanalyze the data reported in this work is available from the lead contact upon reasonable request.

EXPERIMENTAL MODEL AND STUDY PARTICIPANT DETAILS

Animals and protocols

A total of 30 male C57BL/6J mice aged 8 weeks and weighing 20-25 g were purchased from Wuhan Shulaibao Biotechnology Co., Ltd. and used in this study. All mice were housed in a specific pathogen-free (SPF) environment on a 12 h light/dark cycle and were fed a 60% kcal high-fat diet (HFD) (D12492, Shuyushengwu Biotechnology, Shanghai, China). All procedures were approved by the Ethical Approval for Formation Review of Experimental Animal Welfare and Ethics, Zhongnan Hospital of Wuhan University (ZN2023102).

Mice were randomly divided into three groups: NC group (HFD, n = 10), MIE group (HFD + moderate intensity exercise, n = 10), and HIE group (HFD + high intensity exercise, n = 10). A small animal treadmill (SA101, Science Biotechnology, Jiangsu, China) was used for mouse exercise intervention. At the onset of the experiment, all mice underwent a week-long assimilation training program on the treadmill. Each session lasted 30 minutes, with a speed of 5 m/min and a frequency of six sessions per week. Following the assimilation training, the mice in the MIE group received 30-minute sessions of moderate-intensity exercise at a speed of 10 m/min six times a week. Meanwhile, the mice in the HIE group engaged in high-intensity exercise for 30 minutes per session, at a speed of 20 m/min, six times a week. Moreover, the body weight of mice in each group was measured on a weekly basis, and ultrasonic cardiogram (VINNO, Jiangsu) was utilized to assess the ejection fraction (EF) and fractional shortening (FS) of the mice every four weeks.

After eight weeks of training, the mice were euthanized using an overdose of 1% pentobarbital sodium. Blood samples were collected from the retro-orbital sinuses of the mice into Eppendorf tubes and then centrifuged to obtain the plasma, which was subsequently frozen at -80°C. Additionally, the hearts, spleens, and aortas of the mice were collected for histological and immunohistochemical staining, as well as western blotting. Moreover, a portion of the spleen was sent for 16S rRNA sequencing. It is important to highlight that after euthanizing the mice, the mice were immersed in 75% ethanol for 5 minutes. Subsequently, the mice were dissected, and the aforementioned tissues were immediately collected on a clean bench to avoid contamination.

Microbiota transplantation

Lactobacillus johnsonii solution (DSM 10533) was purchased from Mingzhou Biotechnology Co., Ltd. (BMZ133557) and then stored at 4°C in an anaerobic bag.

To verify the effect of *Lactobacillus johnsonii* on Treg production, we conducted the following study. First, we treated the mice with an antibiotic cocktail (0.5 g/L vancomycin, 1 g/L neomycin sulphate, 1 g/L metronidazole, 1 g/L ampicillin) in the drinking water for 4 weeks to clear any existing bacteria. Then, we administered a daily dose of 1 x 10^8 CFU/ml *Lactobacillus johnsonii* to the mice for one month via gavage. We measured the level of Treg cells in the spleen using flow cytometry analysis. The mice were randomly divided into three groups: the control group (receiving 180 μl of PBS via gavage, n = 5), the Lacto group (receiving 180 μl of *Lactobacillus johnsonii* via gavage, n = 5), and the inactive Lacto group (receiving 180 μl of heat-killed *Lactobacillus johnsonii* via gavage, n = 5).

16S rRNA sequence

Spleen bacterial DNA was extracted, and the 16S rRNA gene was sequenced by Personalbio Technology Co., Ltd. (Shanghai, China). Briefly, approximately 80 mg of spleen sample per mouse was collected, and DNA was extracted by a QIAamp DNA Mini Kit (51304, QIAGEN, Hilden, Germany) based on the manufacturer's protocol. Then, a NanoDrop 2000 (Thermo Scientific) was used to evaluate the DNA concentration and purity. The primers (forwards primer: ACTCCTACGGGAGGCAGCA, reverse primer: GGACTACHVGGGTWTCTAAT) were used to amplify the V3-V4 hypervariable regions of the 16S rRNA gene from the DNA extracts. The Illumina NovaSeq 6000 PE 250 system was utilized to sequence the samples and obtain raw data. The raw data underwent denoising using QIIME2 and DADA2, resulting in the generation of clean amplicon sequence variants (ASVs) or operational taxonomic units (OTUs). QIIME2 (version 2019.4) was employed to annotate each ASV/OTU sequence, compute the alpha diversity index, perform beta diversity analysis, and conduct random forest analysis. R software (version 4.0.2) was utilized for various tasks, including drawing rank abundance curves (using the R ggplot2 package), conducting principal coordinate analysis (PCoA) (with the R ape package), generating heatmaps of genus abundance (using the R pheatmap package), and conducting pairwise comparisons of sample groups using the MetagenomeSeq method (via the R metagenomeSeq package).

METHOD DETAILS

Measurement of TC, TG, and LDL-C

Each mouse's plasma was sent to Baiqiandu Biotechnology (Wuhan, China) to measure the levels of total cholesterol (TC), triglyceride (TG), and low-density lipoprotein C (LDL-C).

Transmission electron microscopy (TEM) analysis

Each mouse spleen was collected and fixed in 2.5% glutaraldehyde and sent to Baiqiandu Biotechnology (Wuhan, China) for sample preparation and image acquisition.

Histological and immunohistochemical staining

Mouse samples were harvested for histological analysis after anesthesia with 1% pentobarbital sodium. The heart, aortic and spleen specimens were incubated in 4% formalin for 24 h, paraffin embedded, and cut into 5-μm sections. Five consecutive sections from each heart or aortic specimen were prepared for hematoxylin and eosin (H&E) staining, elastic van Gieson (EVG) staining, Masson trichrome staining and immunostaining (Foxp3, TNF-α and Mac2). Medial elastic layer destruction was graded as I (mild) to IV (severe). The images were acquired using a Leica microscope with a 40× objective and analyzed using Image J software.

Western blotting

A PRO-PREP protein extraction kit (Intron Biotechnology, USA) was used to extract protein from the homogenized heart or aortic tissues, and the extract was then used for western blotting. Total protein was boiled in sample buffer (200 mmol/l Tris [pH 6.8], 20% glycerol, 2% sodium dodecyl sulfate (SDS), 0.1% bromophenol blue, and 10% β-ME), and equal amounts of protein were loaded onto a 10% SDS-polyacrylamide gel. After electrophoresis at 100 V for 1 h to ensure that proteins were transferred onto the nitrocellulose membrane filter, the membrane was then blocked with 4% nonfat dry milk in Tris-buffered saline (TBS) and incubated overnight with primary antibodies against COL1 (72026S, CST, 1:1000), ANP (abs123943, Absin, Shanghai, China, 1:1000), BNP (A2179, ABclonal, Wuhan, China, 1:1000), Foxp3 (A4953, ABclonal, Wuhan, China, 1:1000) and TNF-α (A0277, ABclonal, Wuhan, China, 1:1000). Then, the membranes were washed and incubated for 1 h at room temperature with horseradish peroxidase-labelled species-appropriate secondary antibodies (Cedarlane, Canada). An enhanced chemiluminescence (ECL) kit (GE Healthcare) was used to develop the blots, and the bands were quantified by scanning densitometry with ImageJ software. Finally, intergroup analyses were performed for relative protein levels (GAPDH ratio).

Flow cytometry analysis

Treg cell enrichment was assessed using fluorescence-activated cell sorting (FACS) with a flow cytometer (BD Fortessa; BD Biosciences, San Jose, CA, USA) and analyzed with FlowJo software (FlowJo, Ashland, OR, USA) following labelling of Treg cells with phycoerythrin (PE)-anti-rat Foxp3 monoclonal antibody (A4953, ABclonal, Wuhan, China). The results are expressed as the mean fluorescence intensity.

QUANTIFICATION AND STATISTICAL ANALYSIS

GraphPad Prism 9 (GraphPad Software, La Jolla, CA) was used for statistical analysis, the data are presented as the means ± SDs. P values < 0.05 was considered statistically significant. One-way analysis of variance (ANOVA) using the Bonferroni correction was suitable for comparing multiple groups.